INTERNATIONAL JOURNAL OF
NUMERICAL ANALYSIS AND MODELING
Volume 14, Number 4-5, Pages 712–729

AN AUGMENTED IIM & PRECONDITIONING TECHNIQUE FOR JUMP EMBEDDED BOUNDARY CONDITIONS

PHILIPPE ANGOT[1] AND ZHILIN LI[2]

Abstract. A second-order accurate augmented method is proposed and analyzed in this paper for a general elliptic PDE with a general boundary condition using the jump embedded boundary conditions (JEBC) formulation. First of all, the existence and uniqueness of an interface problem with given are discussed. Then, the well-posedness theory is extended to the interface problems with given jump conditions. In the proposed numerical method, one novel idea is to preconditioning the PDE first so that the coefficient of the highest derivative is of $O(1)$. The second idea is to introduce two augmented variables corresponding to the jump in the solution and its normal derivative along the boundary to get an interface problem. For a piecewise constant coefficient, the fast Poisson solver then can be utilized in a rectangular domain. The augmented variables can be determined from a Schur complement system. We also propose two preconditioning techniques for the GMRES iterative method for the Schur complement; one is from the flux jump condition, and the other one is from the algebraic preconditioner based on the interpolation scheme in the augmented algorithm. The presented numerical results show that the proposed method has not only obtained second order accurate solutions in the L^∞ norm globally, but also second order accurate normal derivatives at the boundary from each side of the interface. The proposed preconditioning technique can speed up 50-90% compared with the method without preconditioning.

Key words. Jump embedded boundary conditions (JEBC), augmented immersed interface method, fast Poisson solver, irregular domain, PDE and algebraic preconditioner.

1. Introduction and mathematical formulation

Let $\Omega \subset \mathbb{R}^d$ ($d{=}2$ or 3 in practice) be an open bounded and connected set with a Lipschitz continuous boundary $\Gamma := \partial\Omega$, and $\boldsymbol{\nu}$ be the outward unit normal vector on Γ. The domain Ω is composed of two disjoint Lipschitz subdomains, the interior domain Ω^- and the exterior one Ω^+ separated by a Lipschitz continuous interface $\Sigma \subset \mathbb{R}^{d-1}$ such that $\Omega = \Omega^- \cup \Sigma \cup \Omega^+$, as shown in Figure 1. The extension to several closed interfaces is straightforward. The case of more general situations when Σ cuts Γ can be treated as well but it is more technical and we refer to [9] for the trace theory. Let $\boldsymbol{n}$ be the unit normal vector on the interface Σ arbitrarily oriented from Ω^- to Ω^+.

We use the standard notations for the Lebesgue and Sobolev spaces, e.g. [8, 15]. In particular, $\|.\|_{0,\Omega}$ denotes the $L^2(\Omega)$-norm, $\|.\|_{1,\Omega}$ the $H^1(\Omega)$-norm, $\|.\|_{-1,\Omega}$ for the $H^{-1}(\Omega)$-norm, $(.,.)_{0,\Omega}$ for the $L^2(\Omega)$-inner product, and $\langle .,. \rangle_{-1,\Omega}$ for the duality pairing between $H^{-1}(\Omega)$ and $H^1_0(\Omega)$ or $\langle .,. \rangle_{-1/2,\Sigma}$ for the duality pairing between $H^{-1/2}(\Sigma)$ and $H^{1/2}(\Sigma)$. We also define the Hilbert spaces below with their usual

Received by the editors on December 31, 2016, accepted on March 20, 2017.

1991 *Mathematics Subject Classification.* 65F08,65N06, 65N85.

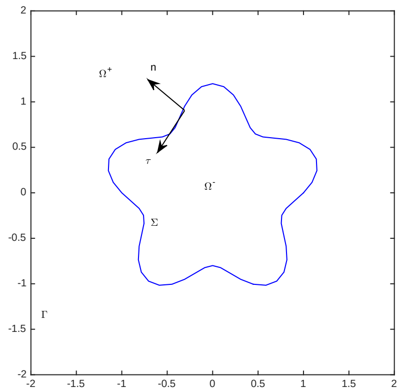

FIGURE 1. Configuration of the interface problem with a closed surface Σ bordering the subdomain Ω^- and $\Omega = \Omega^- \cup \Sigma \cup \Omega^+$. The domain and the interface are used in the numerical experiments.

respective inner products and associated norms:

$$\boldsymbol{H}_{div}(\Omega) = \left\{ \boldsymbol{u} \in L^2(\Omega)^d;\ \boldsymbol{\nabla \cdot u} \in L^2(\Omega) \right\},$$
$$H^1_{0\Gamma}(\Omega) = \left\{ u \in H^1(\Omega);\ u = 0 \text{ on } \Gamma \right\}.$$

For any quantity ψ defined all over Ω, the restrictions on Ω^- or Ω^+ are respectively denoted by $\psi^- := \psi_{|\Omega^-}$ and $\psi^+ := \psi_{|\Omega^+}$. For a function ψ having a jump on Σ, let $\psi^-_{|\Sigma}$ and $\psi^+_{|\Sigma}$ be the traces of ψ^- and ψ^+ on each side of Σ (at least defined in a weak sense), respectively. Following the general framework defined in [3] for scalar elliptic problems with jump interface conditions or its extension to vector problems in [4], let us define the jump of ψ on Σ oriented by $\boldsymbol{n}$ and the arithmetic mean of traces of ψ by :

$$[\![\psi]\!]_\Sigma := \left(\psi^+ - \psi^-\right)_{|\Sigma}, \quad \text{and} \quad \overline{\psi}_\Sigma := \frac{1}{2}\left(\psi^+ + \psi^-\right)_{|\Sigma}.$$

Thus we have also :

$$\psi^+_{|\Sigma} = \overline{\psi}_\Sigma + \frac{1}{2}[\![\psi]\!]_\Sigma, \quad \text{and} \quad \psi^-_{|\Sigma} = \overline{\psi}_\Sigma - \frac{1}{2}[\![\psi]\!]_\Sigma.$$

The interest for choosing such reduced quantities $[\![\psi]\!]_\Sigma$ and $\overline{\psi}_\Sigma$ will appear later with the weak formulation. Let us already notice that when $[\![\psi]\!]_\Sigma = 0$, then we have continuous traces across Σ and $\overline{\psi}_\Sigma = \psi^-_{|\Sigma} = \psi^+_{|\Sigma} = \psi_{|\Sigma}$.

1.1. The classical interface problem with given jumps. The standard scalar elliptic problem considered by Immersed Interface Methods (IIM) [13] reads as follows where the jumps of both the solution and normal flux are given on Σ:

$$
\left\{
\begin{aligned}
-\boldsymbol{\nabla}\boldsymbol{\cdot}(\boldsymbol{a}\nabla u) &= f \quad \text{in } \Omega^- \cup \Omega^+, \\
u &= 0 \quad \text{on } \Gamma, \\
[\![u]\!]_\Sigma &= U \quad \text{on } \Sigma, \\
[\![(\boldsymbol{a}\nabla u)\boldsymbol{\cdot}\boldsymbol{n}]\!]_\Sigma &= \phi \quad \text{on } \Sigma.
\end{aligned}
\right.
\tag{1}
$$

The diffusion tensor $\boldsymbol{a} \in L^\infty(\Omega)^{d\times d}$ is bounded, symmetric and uniformly positive definite, *i.e.* there exists $a_0 > 0$ such that:

$$
(\boldsymbol{a}(x)\,\boldsymbol{\xi})\boldsymbol{\cdot}\boldsymbol{\xi} \geq a_0\,|\boldsymbol{\xi}|^2, \qquad \text{for all } \boldsymbol{\xi} \in \mathbb{R}^d, \qquad \text{for a.e. } x \in \Omega,
$$

where $|.|$ denotes the Euclidean norm in $\mathbb{R}^d$.

Let us recall the solvability result of this problem by considering the Hilbert space:

$$
W := \left\{u \in L^2(\Omega);\ u^- = u_{|\Omega^-} \in H^1(\Omega^-),\, u^+ = u_{|\Omega^+} \in H^1_{0\Gamma}(\Omega^+)\right\},
$$

equipped with the Hilbertian norm (and associated natural inner product) defined by:

$$
\|u\|_W^2 := \|u\|_{0,\Omega}^2 + \|\nabla u\|_{0,\Omega^-}^2 + \|\nabla u\|_{0,\Omega^+}^2, \quad \forall u \in W.
$$

Theorem 1.1 (Well-posedness of the interface problem (1) with jumps). *With the data $f \in L^2(\Omega)$, $U \in H^{1/2}(\Sigma)$ and $\phi \in H^{-1/2}(\Sigma)$, the problem (1) admits a unique solution $u \in W$.*

When $U = 0$, the solution u belongs to $H^1_0(\Omega)$ and satisfies the weak form below for all $\varphi \in H^1_0(\Omega)$:

$$
\int_{\Omega^-} (\boldsymbol{a}\nabla u)\boldsymbol{\cdot}\nabla\varphi\,\mathrm{d}x + \int_{\Omega^+} (\boldsymbol{a}\nabla u)\boldsymbol{\cdot}\nabla\varphi\,\mathrm{d}x = \int_\Omega f\,\varphi\,\mathrm{d}x - \langle\phi,\varphi\rangle_{-1/2,\Sigma}\,. \tag{2}
$$

Proof.

<u>*i) Existence and uniqueness for the case $U = 0$.*</u>

With $f \in L^2(\Omega)$ and $u \in H^1(\Omega)$, since the surface Σ is closed completely bordering Ω^-, we have $(\boldsymbol{a}\nabla u)^\pm \in \boldsymbol{H}_{div}(\Omega^\pm)$ and thus $(\boldsymbol{a}\nabla u)^\pm$ admit normal traces defined in a weak sense $(\boldsymbol{a}\nabla u)\boldsymbol{\cdot}\boldsymbol{n}^\pm_{|\Sigma} \in H^{-1/2}(\Sigma)$ on both sides of the interface Σ; see e.g. [9].
Then, taking the L^2-inner product of the Poisson equation in problem (1) over the subdomains Ω^- and Ω^+ and using Green's formula, we get respectively for any test function $\varphi \in H^1_0(\Omega)$ since $[\![\varphi]\!]_\Sigma = 0$ and $\varphi_{|\Sigma} \in H^{1/2}(\Sigma)$:

$$
\begin{aligned}
\int_{\Omega^-} (\boldsymbol{a}\nabla u)\boldsymbol{\cdot}\nabla\varphi\,\mathrm{d}x - \Big\langle(\boldsymbol{a}\nabla u)\boldsymbol{\cdot}\boldsymbol{n}^-_{|\Sigma},\varphi\Big\rangle_{-1/2,\Sigma} &= \int_{\Omega^-} f\,\varphi\,\mathrm{d}x, \\
\int_{\Omega^+} (\boldsymbol{a}\nabla u)\boldsymbol{\cdot}\nabla\varphi\,\mathrm{d}x + \Big\langle(\boldsymbol{a}\nabla u)\boldsymbol{\cdot}\boldsymbol{n}^+_{|\Sigma},\varphi\Big\rangle_{-1/2,\Sigma} &= \int_{\Omega^+} f\,\varphi\,\mathrm{d}x.
\end{aligned}
$$

By summing the two previous equalities, we have for all $\varphi \in H^1_0(\Omega)$:

$$
\begin{aligned}
\int_{\Omega^-} (\boldsymbol{a}\nabla u)\boldsymbol{\cdot}\nabla\varphi\,\mathrm{d}x &+ \int_{\Omega^+} (\boldsymbol{a}\nabla u)\boldsymbol{\cdot}\nabla\varphi\,\mathrm{d}x \\
&+ \langle[\![(\boldsymbol{a}\nabla u)\boldsymbol{\cdot}\boldsymbol{n}]\!]_\Sigma,\varphi\rangle_{-1/2,\Sigma} = \int_{\Omega^-\cup\Omega^+} f\,\varphi\,\mathrm{d}x.
\end{aligned}
\tag{3}
$$

Now, introducing the given normal flux jump $\phi \in H^{-1/2}(\Sigma)$, it appears that any solution u to the problem (1) satisfies the weak form (2).

Then, as an easy consequence of the Lax-Milgram theorem with Poincaré inequality, there exists a unique solution $u \in H^1_0(\Omega)$ satisfying the weak form (2).

Conversely, let us consider $u \in H^1_0(\Omega)$, with thus $[\![u]\!]_\Sigma = 0$, and verifying (2). By choosing in (2) any test function $\varphi \in H^1_0(\Omega)$ such that $\varphi^- \in H^1_0(\Omega^-)$ extended by $\varphi^+ = 0$, it appears immediately using a standard integration by part that u^- satisfies the Poisson equation of (1) in Ω^-. Similarly, choosing any $\varphi \in H^1_0(\Omega)$ such that $\varphi^+ \in H^1_0(\Omega^+)$ and $\varphi^- = 0$, shows that u^+ verifies the Poisson equation of (1) in Ω^+. Thus, u satisfies the Poisson equation of (1) in the L^2 sense and the weak form (3) holds for all $\varphi \in H^1_0(\Omega)$.

It remains to recover the flux jump equation on Σ. By considering the difference between the equations (3) and (2), we get:

$$\langle [\![(\boldsymbol{a}\nabla u)\boldsymbol{\cdot}\boldsymbol{n}]\!]_\Sigma, \varphi\rangle_{-1/2,\Sigma} = \langle \phi, \varphi\rangle_{-1/2,\Sigma}\,, \quad \forall \varphi \in H^1_0(\Omega).$$

It yields finally that u satisfies the equation for the given normal flux jump on Σ:

$$[\![(\boldsymbol{a}\nabla u)\boldsymbol{\cdot}\boldsymbol{n}]\!]_\Sigma = \phi \in H^{-1/2}(\Sigma).$$

Indeed, any function $\psi \in H^{1/2}(\Sigma)$ can be interpreted as the trace on Σ of a function $\varphi \in H^1_0(\Omega)$. It suffices to define $\varphi \in H^1_0(\Omega)$ by its restrictions φ^- and φ^+ as the solutions of the Dirichlet problems in Ω^- and Ω^+ respectively and verifying $[\![\varphi]\!]_\Sigma = 0$:

$$\begin{cases} \Delta\varphi = 0 & \text{in } \Omega^- \cup \Omega^+, \\ \varphi = 0 & \text{on } \Gamma, \\ \varphi^-_{|\Sigma} = \varphi^+_{|\Sigma} = \psi & \text{on } \Sigma. \end{cases}$$

Thus, we have proved that the unique solution $u \in H^1_0(\Omega)$ to the weak form (2) satisfies the problem (1).

ii) Existence for the general case $U \neq 0$.

Let us construct a suitable extension $v \in W$ of the given function $U \in H^{1/2}(\Sigma)$ such that $[\![v]\!]_\Sigma = U$ on Σ. That will hold by considering the restrictions v^- and v^+ as the solutions of the Dirichlet problems below in Ω^- and Ω^+ respectively:

$$\begin{cases} -\boldsymbol{\nabla}\boldsymbol{\cdot}(\boldsymbol{a}\nabla v^+) = f^+ & \text{in } \Omega^+, \\ v^+ = 0 & \text{on } \Gamma, \\ v^+\big|_\Sigma = U/2 & \text{on } \Sigma. \end{cases} \tag{4}$$

$$\begin{cases} -\boldsymbol{\nabla}\boldsymbol{\cdot}(\boldsymbol{a}\nabla v^-) = f^- & \text{in } \Omega^-, \\ v^-\big|_\Sigma = -U/2 & \text{on } \Sigma. \end{cases} \tag{5}$$

There exists a unique solution $v^+ \in H^1_{0\Gamma}(\Omega^+)$ to the non-homogeneous Dirichlet problem (4). Similarly, there exists a unique solution $v^- \in H^1(\Omega^-)$ to the non-homogeneous Dirichlet problem (5). Hence, this defines a function $v \in W$ all over Ω verifying $[\![v]\!]_\Sigma = U$ on Σ with $(\boldsymbol{a}\nabla v)\boldsymbol{\cdot}\boldsymbol{n}^\pm_{|\Sigma} \in H^{-1/2}(\Sigma)$ since $f \in L^2(\Omega)$ and thus $[\![(\boldsymbol{a}\nabla v)\boldsymbol{\cdot}\boldsymbol{n}]\!]_\Sigma \in H^{-1/2}(\Sigma)$.

Then, we consider the difference $w := u - v$ where u satisfies (1). Using the linearity of the problem, w necessarily satisfies by construction $[\![w]\!]_\Sigma = 0$ and the problem below:

$$\begin{cases} -\boldsymbol{\nabla}\boldsymbol{\cdot}(\boldsymbol{a}\nabla w) = 0 & \text{in } \Omega^- \cup \Omega^+, \\ w = 0 & \text{on } \Gamma, \\ [\![w]\!]_\Sigma = 0 & \text{on } \Sigma, \\ [\![(\boldsymbol{a}\nabla w)\boldsymbol{\cdot}\boldsymbol{n}]\!]_\Sigma = \phi - [\![(\boldsymbol{a}\nabla v)\boldsymbol{\cdot}\boldsymbol{n}]\!]_\Sigma & \text{on } \Sigma. \end{cases} \tag{6}$$

Since now $(\phi - [\![(\boldsymbol{a}\nabla v)\boldsymbol{\cdot}\boldsymbol{n}]\!]_\Sigma)$ belongs to $H^{-1/2}(\Sigma)$ and $[\![w]\!]_\Sigma = 0$, it results from the first part *i)* that the problem (6) admits a unique solution $w \in H_0^1(\Omega)$.

Hence, we have constructed as least one solution $u \in W$ to problem (1) by defining $u := v + w$.

iii) Uniqueness.

Let us suppose that there exists two solutions u and v in W to the problem (1). Then, with the linearity of the problem, the difference $w := u - v$ satisfies the same problem with null data:

$$\begin{cases} -\boldsymbol{\nabla}\boldsymbol{\cdot}(\boldsymbol{a}\nabla w) = 0 & \text{in } \Omega^- \cup \Omega^+, \\ w = 0 & \text{on } \Gamma, \\ [\![w]\!]_\Sigma = 0 & \text{on } \Sigma, \\ [\![(\boldsymbol{a}\nabla w)\boldsymbol{\cdot}\boldsymbol{n}]\!]_\Sigma = 0 & \text{on } \Sigma. \end{cases}$$

This immediately gives $w = 0$ and thus $u = v$, which ends the proof. □

1.2. The interface problem with JEBC.

The so-called Jump Embedded Boundary Conditions (JEBC) were introduced in [2, 3] in order to generalize the interface problem (1) with given jumps. They still consider jumps of both the solution and normal flux on Σ, but they are no longer explicitly given and formulated using the reduced quantities $[\![\psi]\!]_\Sigma$ and $\overline{\psi}_\Sigma$ for the solution and normal flux.

The scalar elliptic problem with JEBC on Σ reads:

$$\begin{cases} -\boldsymbol{\nabla}\boldsymbol{\cdot}(\boldsymbol{a}\nabla u) = f & \text{in } \Omega^- \cup \Omega^+, \\ u = 0 & \text{on } \Gamma, \\ [\![(\boldsymbol{a}\nabla u)\boldsymbol{\cdot}\boldsymbol{n}]\!]_\Sigma = \alpha\,\overline{u}_\Sigma + g & \text{on } \Sigma\,, \\ \overline{(\boldsymbol{a}\nabla u)\boldsymbol{\cdot}\boldsymbol{n}}_\Sigma = \gamma\,[\![u]\!]_\Sigma + z & \text{on } \Sigma\,. \end{cases} \tag{7}$$

Here, $f \in L^2(\Omega)$ is given as well as the data on Σ: the positive and bounded functions $0 \le \alpha,\, \gamma \in L^\infty(\Sigma)$ and $g,\, z \in H^{-1/2}(\Sigma)$.

In the special case with $\alpha = \gamma = 0$, the problem (7) amounts to solve a mixed Dirichlet-Neumann problem in Ω^+ and a pure Neumann problem in Ω^- with $(\boldsymbol{a}\nabla u)\boldsymbol{\cdot}\boldsymbol{n}^-_{|\Sigma} = z - g/2$. Thus, the latter problem requires the usual compatibility condition of the data:

$$\langle z - g/2, 1\rangle_{-1/2,\Sigma} + \int_{\Omega^-} f^-\,\mathrm{d}x = 0,$$

to get a unique solution $u^- \in H^1(\Omega^-)/\mathbb{R}$ up to an additive constant.

Following [2, 3], let us give a nice weak form of problem (7) in the Hilbert space W. It is useful here to introduce on W the following suitable norms and associated inner products:

$$\|u\|_W^2 := \|\nabla u^-\|_{0,\Omega^-}^2 + \|\nabla u^+\|_{0,\Omega^+}^2 + \|[\![u]\!]_\Sigma\|_{0,\Sigma}, \quad \forall u \in W$$

$$\text{or} \qquad \|u\|_W^2 := \|\nabla u^-\|_{0,\Omega^-}^2 + \|\nabla u^+\|_{0,\Omega^+}^2 + \|\overline{u}_\Sigma\|_{0,\Sigma}, \quad \forall u \in W$$

Indeed, it is an easy matter to show that each of them defines an Hilbertian norm on W using the Poincaré inequality in the subdomain Ω^+.

Using Green's formula in Ω^- and Ω^+ respectively, we have for a solution $u \in W$ of problem (7) and for all $\varphi \in W$:

$$\int_{\Omega^-} (\boldsymbol{a}\nabla u)\cdot \nabla\varphi \, \mathrm{d}x - \left\langle (\boldsymbol{a}\nabla u)\cdot \boldsymbol{n}^-_{|\Sigma}, \varphi^-_{|\Sigma} \right\rangle_{-1/2,\Sigma} = \int_{\Omega^-} f\,\varphi \, \mathrm{d}x,$$
$$\int_{\Omega^+} (\boldsymbol{a}\nabla u)\cdot \nabla\varphi \, \mathrm{d}x + \left\langle (\boldsymbol{a}\nabla u)\cdot \boldsymbol{n}^+_{|\Sigma}, \varphi^+_{|\Sigma} \right\rangle_{-1/2,\Sigma} = \int_{\Omega^+} f\,\varphi \, \mathrm{d}x.$$

We sum up these equations using the key "$\pm$ equality" below:

(8)
$$\left\langle (\boldsymbol{a}\nabla u)\cdot \boldsymbol{n}^+_{|\Sigma}, \varphi^+_{|\Sigma} \right\rangle_{-1/2,\Sigma} - \left\langle (\boldsymbol{a}\nabla u)\cdot \boldsymbol{n}^-_{|\Sigma}, \varphi^-_{|\Sigma} \right\rangle_{-1/2,\Sigma}$$
$$= \langle [\![(\boldsymbol{a}\nabla u)\cdot \boldsymbol{n}]\!]_\Sigma, \overline{\varphi}_\Sigma \rangle_{-1/2,\Sigma} + \left\langle \overline{(\boldsymbol{a}\nabla u)\cdot \boldsymbol{n}}_\Sigma, [\![\varphi]\!]_\Sigma \right\rangle_{-1/2,\Sigma}.$$

Then, we get:

$$\begin{aligned} &\int_{\Omega^-} (\boldsymbol{a}\nabla u)\cdot \nabla\varphi \, \mathrm{d}x + \int_{\Omega^+} (\boldsymbol{a}\nabla u)\cdot \nabla\varphi \, \mathrm{d}x \\ &\qquad + \langle [\![(\boldsymbol{a}\nabla u)\cdot \boldsymbol{n}]\!]_\Sigma, \overline{\varphi}_\Sigma \rangle_{-1/2,\Sigma} + \left\langle \overline{(\boldsymbol{a}\nabla u)\cdot \boldsymbol{n}}_\Sigma, [\![\varphi]\!]_\Sigma \right\rangle_{-1/2,\Sigma} \\ &\qquad = \int_{\Omega^-\cup\Omega^+} f\,\varphi \, \mathrm{d}x, \qquad \text{for all } \ \varphi \in W. \end{aligned} \tag{9}$$

Now inputting the jump interface conditions JEBC on Σ and using the continuous embedding $H^{1/2}(\Sigma) \hookrightarrow L^2(\Sigma) \hookrightarrow H^{-1/2}(\Sigma)$, it yields the weak form of problem (7) in W:

(10)
$$\begin{aligned} &\int_{\Omega^-} (\boldsymbol{a}\nabla u)\cdot \nabla\varphi \, \mathrm{d}x + \int_{\Omega^+} (\boldsymbol{a}\nabla u)\cdot \nabla\varphi \, \mathrm{d}x \\ &\qquad + \int_\Sigma \alpha\, \overline{u}_\Sigma\, \overline{\varphi}_\Sigma \, \mathrm{d}s + \int_\Sigma \gamma\, [\![u]\!]_\Sigma\, [\![\varphi]\!]_\Sigma \, \mathrm{d}s \\ &\qquad = \int_{\Omega^-\cup\Omega^+} f\,\varphi \, \mathrm{d}x - \langle g, \overline{\varphi}_\Sigma \rangle_{-1/2,\Sigma} - \langle z, [\![\varphi]\!]_\Sigma \rangle_{-1/2,\Sigma}, \quad \forall \varphi \in W. \end{aligned}$$

Let us prove for completeness the solvability result of problem (7), excluding the particular case when $\alpha = \gamma = 0$ for sake of shortness.

Theorem 1.2 (Well-posedness of the interface problem (7) with JEBC). *With the data $f \in L^2(\Omega)$, g, $z \in H^{-1/2}(\Sigma)$ and $0 \le \alpha$, $\gamma \in L^\infty(\Sigma)$ (excluding the particular case $\alpha = \gamma = 0$), the problem (7) admits a unique solution $u \in W$ which* *satisfies the weak problem (10) and the following energy equality:*

$$\int_{\Omega^-\cup\Omega^+} (\boldsymbol{a}\nabla u)\cdot\nabla u\,\mathrm{d}x + \int_\Sigma \alpha\,|\overline{u}_\Sigma|^2\,\mathrm{d}s + \int_\Sigma \gamma\,|[\![u]\!]_\Sigma|^2\,\mathrm{d}s$$
$$= \int_{\Omega^-\cup\Omega^+} f\,u\,\mathrm{d}x - \langle g, \overline{u}_\Sigma\rangle_{-1/2,\Sigma} - \langle z, [\![u]\!]_\Sigma\rangle_{-1/2,\Sigma}\,.$$

Moreover, if the data g, r are given in $L^2(\Sigma)$, then we get the extra-regularity of the normal fluxes: $[\![(\boldsymbol{a}\nabla u)\cdot\boldsymbol{n}]\!]_\Sigma$, $\overline{(\boldsymbol{a}\nabla u)\cdot\boldsymbol{n}_\Sigma} \in L^2(\Sigma)$ and thus $(\boldsymbol{a}\nabla u)\cdot\boldsymbol{n}^\pm_{|\Sigma} \in L^2(\Sigma)$.

Proof.

We have already shown that any solution $u \in W$ of problem (7) also satisfies the weak form (10). By applying the Lax-Milgram theorem in W equipped with one of the suitable Hilbertian norms defined above (to deal with the particular cases when $\alpha = 0$ with $\gamma \neq 0$ or $\alpha \neq 0$ with $\gamma = 0$), there exists a unique solution $u \in W$ to the weak problem (10).

Conversely, if $u \in W$ is the solution of (10), we have already $u_{|\Gamma} = 0$, and it is easy to show that u satisfies the Poisson equation of problem (7) in the L^2 sense both in Ω^- and Ω^+. Indeed, it suffices to choose in (10) any test function $\varphi \in H^1_0(\Omega) \subset W$ such that, either $\varphi^- \in H^1_0(\Omega^-)$ extended with $\varphi^+ = 0$, or $\varphi^+ \in H^1_0(\Omega^+)$ with $\varphi^- = 0$. Thus, the weak form (9) also holds since $f \in L^2(\Sigma)$.
It remains to recover the jump interface conditions JEBC on Σ.

By doing the difference between (9) and (10), we have for all $\varphi \in W$:
(11)
$$\langle[\![(\boldsymbol{a}\nabla u)\cdot\boldsymbol{n}]\!]_\Sigma, \overline{\varphi}_\Sigma\rangle_{-1/2,\Sigma} + \left\langle \overline{(\boldsymbol{a}\nabla u)\cdot\boldsymbol{n}}_\Sigma, [\![\varphi]\!]_\Sigma \right\rangle_{-1/2,\Sigma}$$
$$= \langle(\alpha\,\overline{u}_\Sigma + g), \overline{\varphi}_\Sigma\rangle_{-1/2,\Sigma} + \langle(\gamma\,[\![u]\!]_\Sigma + z), [\![\varphi]\!]_\Sigma\rangle_{-1/2,\Sigma}\,.$$

Let us now take any function $\psi \in H^{1/2}(\Sigma)$ and let us consider $\varphi \in H^1_0(\Omega)$ such that $[\![\varphi]\!]_\Sigma = 0$ by definition of $H^1(\Omega)$ and $\overline{\varphi}_\Sigma = \varphi_{|\Sigma} = \psi$ defined by its restrictions φ^- and φ^+ as the solutions of the Dirichlet problems below over Ω^- and Ω^+:

$$\begin{cases} \Delta\varphi = 0 & \text{in } \ \Omega^-\cup\Omega^+, \\ \varphi = 0 & \text{on } \ \Gamma, \\ \varphi^-_{|\Sigma} = \varphi^+_{|\Sigma} = \psi & \text{on } \ \Sigma. \end{cases}$$

Then (11) gives:

$$\langle[\![(\boldsymbol{a}\nabla u)\cdot\boldsymbol{n}]\!]_\Sigma, \psi\rangle_{-1/2,\Sigma} = \langle(\alpha\,\overline{u}_\Sigma + g), \psi\rangle_{-1/2,\Sigma}\,, \quad \forall\psi \in H^{1/2}(\Sigma).$$

Thus, the first jump interface condition of problem (7) is satisfied in the weak sense of $H^{-1/2}(\Sigma)$.

Let us now take $\varphi \in W$ such that $[\![\varphi]\!]_\Sigma = \psi$ with $\overline{\varphi}_\Sigma = 0$ defined by its restrictions φ^- and φ^+ as the solutions of the Dirichlet problems below in Ω^- and Ω^+:

$$\begin{cases} \Delta\varphi = 0 & \text{in } \Omega^- \cup \Omega^+, \\ \varphi = 0 & \text{on } \Gamma, \\ \varphi^+_{|\Sigma} = \psi/2 & \text{on } \Sigma, \\ \varphi^-_{|\Sigma} = -\psi/2 & \text{on } \Sigma. \end{cases}$$

Then (11) gives:

$$\left\langle \overline{(\boldsymbol{a}\nabla u)\cdot \boldsymbol{n}}_\Sigma, \psi \right\rangle_{-1/2,\Sigma} = \langle (\gamma\,[\![u]\!]_\Sigma + z), \psi\rangle_{-1/2,\Sigma}, \quad \forall \psi \in H^{1/2}(\Sigma).$$

Hence, the second jump interface condition of problem (7) is also satisfied in the weak sense of $H^{-1/2}(\Sigma)$, which concludes the proof. □

1.3. Main interests of JEBC.

The jump interface conditions in problem (7) have many interesting features. First, the weak form (10) can be directly exploited for the numerical approximation of (7) with finite elements, extended finite elements, finite volumes with gradient schemes or discontinuous Galerkin methods. We refer for example to the finite volumes scheme proposed and analysed in [2] for an interface-fitted unstructured mesh. This scheme is also numerically experimented for the JEBC with Cartesian grids and nested multi-level mesh refinements, either in the case of a diffuse or spread discrete interface in [17] as for the Immersed BC method [16], or for a sharp interface in [18].

Other interests lie in the different sub-models which can be obtained from problem (7):

a) The choice $\alpha = g = 0$ gives the condition of the imperfect contact on Σ with no flux jump $[\![(\boldsymbol{a}\nabla u)\cdot \boldsymbol{n}]\!]_\Sigma = 0$:

$$(\boldsymbol{a}\nabla u)\cdot \boldsymbol{n}_{|\Sigma} = \gamma\,[\![u]\!]_\Sigma + z \quad \text{on } \Sigma.$$

The perfect transmission is easily recovered with $h = 0$ and a surface penalty $\gamma = 1/\varepsilon$ with $0 < \varepsilon \ll 1$, which gives $[\![u]\!]_\Sigma = 0$ at the limit when $\varepsilon \to 0$; see [3].

b) In the same spirit, the model with flux jumps and no jump of solution is obtained with $z = 0$ and $\gamma = 1/\varepsilon$, which gives $[\![u]\!]_\Sigma = 0$ at the limit when $\varepsilon \to 0$ and the Stefan-like interface condition:

$$[\![(\boldsymbol{a}\nabla u)\cdot \boldsymbol{n}]\!]_\Sigma = \alpha\, u_{|\Sigma} + g \quad \text{on } \Sigma.$$

c) The problem (1) can be also easily recovered from (7) by taking $\alpha = 0$, $g = \phi$, $\gamma = 1/\varepsilon$ with $z = -U/\varepsilon$, which gives $[\![u]\!]_\Sigma = U$ at the limit when $\varepsilon \to 0$; see [4, Theorem 1.2]. By the way, this result gives another proof of existence of solution to problem (1) by passing to the limit in problem (7) when the penalty parameter ε goes to zero.

d) It is also discussed and analysed in [3] how to get the Dirichlet, Neumann, or even the Robin (Fourier) boundary conditions on Σ in the framework of fictitious domain method.

e) The JEBC are naturally generalized in [4] for vector elliptic problems like the Stokes, Brinkman or elasticity problems.

f) The general framework introduced in [4] provides the means to study several jump interface conditions of the velocity and stress vectors for the incompressible viscous flow at a fluid-porous interface. Indeed, the Stokes/Brinkman and Stokes/Darcy problems are theoretically analysed in [5, 6].

In this paper, we apply the augmented immersed interface method (AIIM) based on a finite difference discretization to solve the problem (7) by introducing two augmented variables $q_1 = [\![u]\!]$ and $q_2 = [\![u_n]\!] = [\![\partial_n u]\!]$ so that we can decouple the complicated interface conditions in (7) and to obtained an accurate discretization using the IIM. The augmented variables are only defined along the interface and have co-dimension one compared with that of the solution. The augmented variables should satisfy a Schur complement system that is solved by the GMRES iteration. Both preconditioning techniques based on the continuous form of the problem and an efficient algebraic preconditioner are developed and studied. The preconditioner techniques provide about $50 - 90\%$ speed-up compared with that without preconditioning.

2. The numerical method

For simplicity of the discussion, we assume that the coefficient $\mathbf{a}(\mathbf{x})$ is a piecewise constant,

$$\mathbf{a}(\mathbf{x}) = \begin{cases} \beta^+ & \text{if } \mathbf{x} \in \Omega^+, \\ \beta^- & \text{if } \mathbf{x} \in \Omega^-, \end{cases} \tag{12}$$

and $\mathbf{a}(\mathbf{x}) \geq \beta_0 > 0$. For variable coefficients, the approach should also work with the recent work in [14].

With given augmented variable $q_1 \in C^2(\Sigma)$ and $q_2 \in C^1(\Sigma)$, we precondition the governing PDE (7) and solve the following problem,

$$-\Delta u = \frac{1}{\beta} f(\mathbf{x}), \qquad \mathbf{x} \in \Omega^+ \cup \Omega^- - \Sigma, \tag{13}$$

$$[\![\, u \,]\!]_\Sigma = q_1, \qquad [\![\, \nabla u \cdot \mathbf{n} \,]\!]_\Sigma = q_2. \tag{14}$$

With the immersed interface method [13], this step is equivalent to a fast Poisson solver such as an FFT [1].

The solution $u(\mathbf{x})$ above is a functional of $q_1(\mathbf{X})$ and $q_2(\mathbf{X})$ and can be written as u_{q_1,q_2}. The solution to the original problem (7) is the one with particular choice of (q_1^*, q_2^*) such that

$$[\![\, \beta \nabla u_{q_1^*,q_2^*} \cdot \mathbf{n} \,]\!]_{\mathbf{X}} = \alpha \, \overline{u_{q_1^*,q_2^*}}\big|_{\mathbf{X}} + g(\mathbf{X}), \qquad \mathbf{X} \in \Sigma, \tag{15}$$

$$\overline{\beta \nabla u_{q_1^*,q_2^*} \cdot \mathbf{n}}\,\Big|_{\mathbf{X}} = \gamma [\![u_{q_1^*,q_2^*}]\!]_{\mathbf{X}} + z(\mathbf{X}), \qquad \mathbf{X} \in \Sigma. \tag{16}$$

The (13)-(16) are the continuous version of the augmented method.

2.1. The augmented method in discrete form. Without loss of generality, we assume that $\Omega^+ \cup \Omega^-$ is a rectangular domain $[a\ b] \times [c\ d]$. In discretization, we assume that $b - a = d - c$ for convenience of presentation. Given a parameter N, we set up a uniform Cartesian grid with $h = (b - a)/N$,

$$x_i = a + ih; \quad y_j = c + jh, \qquad i, j = 0, 1, \cdots, N. \tag{17}$$

We use a cubic periodic spline [11] to represent the closed interface by providing a set of control points $\mathbf{X}_k = (X_k, Y_k)$, $k = 1, 2, \cdots, N_b$. Then the augmented variables and the interface conditions are defined and discretized at the control points. With the values at control points for a surface function, we can find the value, the first and second order surface derivatives at any point on the surface with order $O(h_s^3)$ for the function, $O(h_s^2)$ for the first order, and $O(h_s)$ for the second order derivatives, respectively, where h_s is the mesh size of the discretization of the interface and we choose $h_s \sim h$. We also obtain the tangential and normal directions with accuracy of $O(h_s^2)$ and the curvature with accuracy of $O(h_s)$ information of the interface.

With the immersed interface method, given discrete values of q_1 and q_2, we use the standard centered five point finite difference stencil to discretize the PDE at all grid points where the solution is unknown as

$$-\frac{U_{i-1,j} + U_{i+1,j} + U_{i,j-1} + U_{i,j+1} - 4U_{i,j}}{h^2} = \frac{1}{\beta^\pm} f_{i,j} + C_{i,j}, \tag{18}$$

where $U_{i,j} \approx u(x_i, y_j)$ is the finite difference solution at (x_i, y_j), the '+' and '$-$' in $\beta^\pm$ are determined according to the location of the grid point. If a grid point is on the interface, then we pre-define it as on one particular side. At a regular grid point (x_i, y_j), that is, all grid points involved in the finite difference scheme above are from one side of the interface, the correction term $C_{i,j}$ is zero. At an irregular grid point where at least one grid point involved in the finite difference scheme above is from a different side of the interface, the correction term $C_{i,j}$ typically is non-zero and determined from the IIM, see for example, [13]. The correction term $C_{i,j}$ depends on the discrete augmented variables $Q_{1,k} \approx q_1(\mathbf{X}_k)$, $Q_{2,k} \approx q_2(\mathbf{X}_k)$, $k = 1, 2, \cdots N_b$ linearly.

Let us put the discrete solution $\{U_{ij}\}$ together as a vector $\mathbf{U}$ whose dimension is $O(MN)$, where M and N are the number of grid lines in the x- and y- directions, respectively. We denote also the vector of the discrete values of (q_1, q_2) at the control points $\{\mathbf{X}_k\}$ by $\mathbf{Q}$ whose dimension is $O(2N_b)$. Then the discrete solution of (18) given $\mathbf{Q}$ can be written as

$$A\,\mathbf{U} + B\mathbf{Q} = \mathbf{F}_1 \tag{19}$$

for some vector $\mathbf{F}_1$ and sparse matrices A and B.

The next step is to evaluate the residual of the augmented equations (7). This step involves local interpolations and it is equivalent to discretize the interface conditions in (7).

At each control point $\mathbf{X}_l$, we interpolate the discrete solution $\{U_{ij}\}$ to get their values, normal and tangential derivatives from each side of the interface, $U_k^\pm$, $(\frac{\partial U}{\partial n})_k^\pm$, $(\frac{\partial U}{\partial \tau})_k^\pm$ and so on. Note that, for Poisson/Helmholtz equations with known jump conditions in the solution and the normal derivative, the computed solution and first order partial derivatives at grid points are second order accurate with central finite difference schemes plus correction terms, see for example, [7]. From the second order accurate values at grid points, we also get second order accurate values at the control points since the coefficients of the interpolation are $O(1)$.

The discretized residual of the interface conditions (15)-(16) can be written

$$R(\mathbf{Q}) = C\,\mathbf{U} + D\mathbf{Q} - \tilde{\mathbf{F}}_2 \tag{20}$$

for some sparse matrices C and D. The approximate solution $(\mathbf{U}, \mathbf{Q})$ should satisfy $R(\mathbf{Q}) = \mathbf{0}$ and (19), or the following system of equations,

$$\begin{bmatrix} A & B \\ C & D \end{bmatrix} \begin{bmatrix} \mathbf{U} \\ \mathbf{Q} \end{bmatrix} = \begin{bmatrix} \tilde{\mathbf{F}}_1 \\ \tilde{\mathbf{F}}_2 \end{bmatrix}. \tag{21}$$

The Schur complement for $\mathbf{Q}$ is

$$(D - CA^{-1}B)\mathbf{Q} = \tilde{\mathbf{F}}_2 - CA^{-1}\tilde{\mathbf{F}}_1 = \bar{\mathbf{F}}, \qquad \text{or} \qquad S\mathbf{Q} = \bar{\mathbf{F}}, \tag{22}$$

where $A^{-1}\tilde{\mathbf{F}}_1$ is the result of the Poisson solver for a regular problem given the source term $\tilde{\mathbf{F}}_1$. It has been shown in [13] and other related papers, that the matrix-vector multiplication $S\mathbf{Q}$ given $\mathbf{Q}$ is simply

$$S\mathbf{Q} = R(\mathbf{Q}) + \bar{\mathbf{F}} = R(\mathbf{Q}) - R(\mathbf{0}), \tag{23}$$

where $R(\mathbf{Q}) = S\mathbf{Q} - \bar{\mathbf{F}}$. The right hand side of $S\mathbf{Q} = \bar{\mathbf{F}}$ can be computed from $-R(\mathbf{0})$ which corresponds to the residual of the interface condition with zero values of augmented variables, which is the result from the regular Poisson equations on the rectangular domain.

It is time and memory consuming to form those matrices and the Schur complement at each iteration. Instead, we use the GMRES iterative method to solve for $\mathbf{Q}$. The GMRES iterative method only requires the matrix-vector multiplication which contains the two steps: (1) solve for $\mathbf{U}$ from $A\mathbf{U} = \mathbf{F}_1 - B\mathbf{Q}$; (2) compute the residual of the boundary condition $R(\mathbf{Q}) = C\mathbf{U} + D\mathbf{Q} - \mathbf{F}_2$. We skip the details here since they can be found in [12].

2.2. Preconditioning strategies. Because of the general boundary conditions in (7), in general, we do not have fast convergence of the GMRES method. The number of GMRES iterations depends on the geometry and the mesh size. There are several different ways both in continuous and discrete level to precondition the system. Dividing the coefficient from the highest derivative terms in (13) itself is an efficient preconditioning technique in the continuous level.

In [10], an efficient preconditioning strategy is developed for the fast immersed interface method corresponding to the augmented Poisson equation (13)-(16) for interface problems, that is, γ is large and α is small. The idea is to force the flux jump condition as much as we can by using,

$$
\text{If} \quad \beta^+ < \beta^- : \quad \begin{cases} \mathbf{U}_n^+ \ \text{ is determined by an interpolation,} \\ \mathbf{U}_n^- = \dfrac{\mathbf{V} - \beta^+ \mathbf{Q}}{\beta^+ - \beta^-}, \end{cases}
$$
$$
\text{If} \quad \beta^+ > \beta^- : \quad \begin{cases} \mathbf{U}_n^- \ \text{ is determined by an interpolation,} \\ \mathbf{U}_n^+ = \dfrac{\mathbf{V} - \beta^- \mathbf{Q}}{\beta^+ - \beta^-}. \end{cases} \tag{24}
$$

where $\mathbf{V} = \alpha \, \overline{u_{q_1^*, q_2^*}}\big|_{\mathbf{X}} + g(\mathbf{X})$ in discrete form from (7), we refer the readers to [10, 13] for more details. This preconditioning is still quite efficient if γ is large enough so that the original problem is close to a standard interface problem in which we know the jump in the solution and the flux for the elliptic interface problem. However, the preconditioning techniques has only marginal effect for modest or small γ.

In [19], a sophisticated preconditioning technique is developed for the augmented IIM as well as for general linear system of equations. The implementation is non-trivial though. In this paper, we have developed an alternative and simpler algebraic preconditioning technique that takes advantage of the algorithm and structure of the numerical method explained above, which is somewhat similar to right block diagonal preconditioning technique.

Let the dimension of the Schur complement matrix be $N_s \times N_s$ with $N_s = 2N_b$. In the simple preconditioning strategy, we take a parameter L as the number of the targeted block preconditioning, an integer between $10 \sim 30$ such that N_s/L is close to an integer. Also $L/2$ should be close to the number of interpolation grid points involved in discretizing the boundary conditions (15)-(16). Let $N_s = KL+r$, that is, we use K blocks plus remainder r as the left block preconditioning. We construct

$$
\bar{I} = \begin{bmatrix} I_L \\ I_L \\ I_L \\ \vdots \\ I_L \\ \widetilde{I_L} \end{bmatrix}, \qquad \text{where} \quad \widetilde{I_L} = \begin{bmatrix} I_r & \mathbf{0}^{r \times r} \end{bmatrix} \tag{25}
$$

where I_L is the identity matrix of L by L, I_r is the identity matrix of r by r, the zero matrix has dimension of r by $L - r$. Let

$$
\bar{P} = S\bar{I} = \begin{bmatrix} B_1 \\ B_2 \\ B_3 \\ \vdots \\ B_K \\ \widetilde{B_r} \end{bmatrix}, \tag{26}
$$

where $\widetilde{B_r} = [B_r,\ \bar{B}_{L-r}]$ and B_r is an n_r by n_r matrix. To get B_i, only matrix and vector multiplications are needed. Then we define the preconditioning matrix as

$$P^{-1} = \begin{bmatrix} B_1^{-1} & & & & & \\ & B_2^{-1} & & & & \\ & & B_3^{-1} & & & \\ & & & \ddots & & \\ & & & & B_K^{-1} & \\ & & & & & B_r^{-1} \end{bmatrix} \tag{27}$$

The new system of equations is $P^{-1}\mathcal{S}\,Q = P^{-1}\bar{\mathbf{F}}$.

The preconditioning technique works well for elliptic and parabolic problems because that the diagonal blocks are close to the identity matrices after the preconditioning while the magnitudes of off-diagonal blocks decay like $O(1/r)$, or a $O(1/\log r)$ away from the diagonal using the fundamental solutions of elliptic and parabolic equations. In Table 1-3 (b) and Table 4, we list a comparison of the number of GMRES iterations from one of examples. We can see that the number of GMRES iterations is significantly reduced with suitable choice of L.

3. Numerical experiments

We use a general example to show the efficiency of the augmented method. The computational domain is $[-2,\ 2] \times [-2,\ 2]$. We present errors in L^∞ norms and estimate the convergence order using

$$p = \frac{1}{\log 2} \log \frac{\|\mathbf{E}_{2h}\|_\infty}{\|\mathbf{E}_h\|_\infty}.$$

The tolerance of the GMRES iteration is set to be 10^{-8} and the initial value is set to be $\mathbf{0}$ in all computations. The interface Σ is expressed using the cubic spline package [11],

$$r_\Sigma = r_0 + 0.1\sin(5\theta), \qquad 0 \le \theta < 2\pi. \tag{28}$$

The analytic solution is chosen as

$$u(x,y) = \begin{cases} x^2 - y^2 & \text{in } \Omega^-, \\ \sin(x)\cos(y) & \text{in } \Omega^+, \end{cases} \tag{29}$$

The source term is then determined as

$$f(x,y) = \begin{cases} 0, & \text{in } \Omega^-, \\ -2\beta^+ \sin x \cos y & \text{in } \Omega^+, \end{cases} \tag{30}$$

The jump in the solution, the jump in the flux, the average of the solutions, and the flux are

$$
\begin{aligned}
[\![u]\!] &= \sin(X)\cos(Y) - X^2 + Y^2,\\
[\![\beta u_n]\!] &= \beta^+ \left(\cos(X)\cos(Y)\cos\theta - \sin(X)\sin(Y)\sin\theta\right)\\
&\quad - \beta^- \left(2X\cos\theta - 2Y\sin\theta\right),\\
\overline{u} &= \frac{1}{2}\left(X^2 - Y^2 + \sin X\cos Y\right),\\
\overline{\beta u_n} &= \frac{1}{2}\Big(\beta^+ \left(\cos(X)\cos(Y)\cos\theta - \sin(X)\sin(Y)\sin\theta\right)\\
&\quad + \beta^- \left(2X\cos\theta - 2Y\sin\theta\right) \Big),
\end{aligned}
$$

where $\mathbf{n} = (\cos\theta, \sin\theta)$ is the unit normal direction at an interface point (X, Y) pointing to the Ω^+ direction. Then, the function $z(\mathbf{X})$ and $g(\mathbf{X})$ are determined from the analytic solution and given parameters α and γ from the relations (7). The tolerance for the GMRES iteration is taken as $\epsilon = 10^{-8}$. In Fig.2, we show a computed solution from which we can see that the solution is discontinuous across a five-star interface.

TABLE 1. (a) A grid refinement analysis with $\beta^- = 1$, $\beta^+ = 1$, $\alpha = 1$, $\gamma = 0.1$.

N	$E(u)$	p	$E(u_n^-)$	p	$E(u_n^+)$	p
40	1.0790e-02		1.1860e-02		3.6240e-02	
80	7.6510e-04	3.8179	4.0440e-04	4.8742	2.0870e-03	4.1181
160	1.6510e-04	2.2123	9.8680e-05	2.0350	4.5740e-04	2.1899
320	2.8280e-05	2.5455	1.1270e-05	3.1303	6.8080e-05	2.7482
640	6.3860e-06	2.1468	2.6370e-06	2.0955	1.5590e-05	2.1266

(b) The number of iterations without and with the new preconditioning strategy.

N	40	80	160	320	640
No-Pre	46	65	97	142	202
New-Pre	16	25	34	50	83

In Table 1-3 (a), we show the errors of the computed solution $E(u)$ at all grid points, that is, the error in the infinity norm, and errors of the normal derivative $E(u_n^-)$ and $E(u_n^+)$, at the control points $\mathbf{X}_k$ from each side of the interface with different jump of the coefficient β^- and β^+. We set the parameters $\alpha = 1$ and $\gamma = 0.5$. Not only we see more than second order convergency for the solution, but also better than second order convergency for the normal derivative from each side of the interface at the control points of the interface used for the spline interpolation. While it is surprising that the convergence rates are more than second order, we can see the trend that the convergence rates approach number two as we refine the mesh further.

In Table 1-3 (b), we show the number of GMRES iterations for the Schur complement system with and without preconditioning technique. The number of GMRES

TABLE 2. (a), A grid refinement analysis with $\beta^- = 1000$, $\beta^+ = 1$. The average convergence orders are 3.3288, 4.2931, and 4.2812, respectively for the three quantities.

N	$E(u)$	p	$E(u_n^-)$	p	$E(u_n^+)$	p
40	9.3120e-01		8.5460e-03		1.1640e+01	
80	5.2030e-02	4.1617	3.1310e-05	8.0925	4.2750e-02	8.0890
160	2.6230e-02	0.98813	1.7070e-05	0.87516	2.3290e-02	0.87621
320	2.3590e-04	6.7969	1.5360e-07	6.7961	2.3210e-04	6.6488
640	9.1360e-05	1.3685	5.7850e-08	1.4088	8.1450e-05	1.5108

(b) The number of iterations without and with the two preconditioning strategies.

N	40	80	160	320	640
No-Pre	64	102	182	330	512
Pre-(24)	60	88	127	191	277
New-Pre	17	26	37	54	87

iterations is roughly how many fast Poisson solvers are called to obtain the solution globally, and the normal derivative at the interface from each side at the control points.

Although we have preconditioned the partial differential equation by dividing the coefficient from the highest derivative term, without other preconditioning techniques applied, the number of GMRES iteration increases with mesh size and the jump ratio as expected, but not doubled as we refine the mesh indicating that the preconditioning the PDE does help. In the table, Pre-(24) ($\beta^- \neq \beta^+$) is the preconditioning technique from equation (24) proposed in [10] which is still efficient if γ is large corresponding to an interface problem in the traditional definition; New-Pre is the algebraic preconditioning techniques described in this paper with $L = 20$.

TABLE 3. A grid refinement analysis with $\beta^- = 1$, $\beta^+ = 1000$, $\alpha = 1$, $\gamma = 0.1$.

N	$E(u)$	r	$E(u_n^-)$	r	$E(u_n^+)$	r
40	8.1020e-01		5.2620e-01		2.8090e-03	
80	3.1440e-02	4.6876	1.7750e-02	4.8897	1.0180e-04	4.7862
160	6.9890e-04	5.4914	5.3390e-04	5.0551	2.1880e-06	5.5400
320	7.8090e-05	3.1619	4.4300e-05	3.5912	2.1860e-07	3.3232
640	1.2040e-05	2.6973	4.2500e-06	3.3818	2.8000e-08	2.9648

(b) The number of iterations without and with the preconditioning strategy.

N	40	80	160	320	640
No-Pre	66	106	183	343	510
New-Pre	15	23	33	49	82

With the new algebraic preconditioning technique, the number of GMRES iterations is nearly independent of the coefficient, see Table 1-3 (b), and only slightly increases as the mesh gets finer.

TABLE 4. Comparison of number of GMRES iterations with and without the pre-conditioning strategies. $\beta^- = 1000$, $\beta^+ = 1$, $\alpha = 1$, $\gamma = 1000$.

N	40	80	160	320	640
No-Pre	67	117	205	375	637
Pre-(24)	42	46	53	78	118
New-Pre	15	20	26	40	68

In Table 4, we show the comparison of the number of GMRES iterations for large $\gamma = 1000$, for which the problem is close to a classical interface problem given the jump conditions in the solution and the normal derivative. We can see that the preconditioning technique in [10] using the flux jump condition has significantly reduced the number of GMRES iterations. But still, the algebraic preconditioning technique is the best. Of course, the algebraic preconditioning technique is more complicated and require some extra cost in the realization.

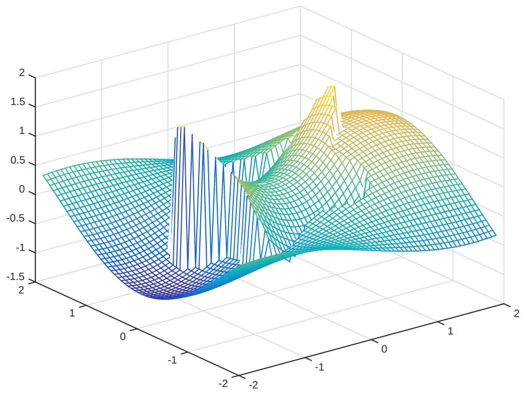

FIGURE 2. The plot of the computed solution with a 60×60 grid. Both the solution and the normal derivative are discontinuous. Using the augmented strategy, we observe second order accurate solution (globally) and the normal derivative at the interface from each side of the interface.

4. Conclusions

In this paper, we proposed an efficient augmented method for solving an elliptic PDE with the JEBC formulations. The advantage of JEBC is the uniform treatment and variational form for a class of boundary value and interface problems. In our proposed augmented method applied to the preconditioned PDE, we introduce two augmented variables as the jump variables of the solution and the normal derivative so that a fast Poisson solver can be utilized for piecewise constant coefficient. The augmented variables are solved through the GMRES iterative method with some new preconditioning techniques. The preconditioning technique uses matrix-vector multiplication only and makes use of the algorithm, that is, the interpolation scheme. The preconditioning technique will be effective in general for elliptic and parabolic problems since the off-diagonal blocks will decay from the fundamental solutions. Numerical experiments show that the proposed method provides not only second-order accuracy for the solution globally, but also second-order accurate normal (or first order partial) derivatives from each side of the interfaces. The preconditioning technique speedup is nearly 50-75%.

Acknowledgements

The second author was partially supported by the US NSF grant DMS-1522768, CNSF grants 11371199, 11471166. The work is partially done during the visit to Aix-Marseille University as a French CNRS senior visiting scientist.

References

[1] J. Adams, P. Swarztrauber, and R. Sweet, Fishpack: Efficient Fortran subprograms for the solution of separable elliptic partial differential equations, http://www.netlib.org/fishpack/.

[2] Ph. Angot, A model of fracture for elliptic problems with flux and solution jumps, C. R. Acad. Sci. Paris, Serie I Math. 337 (2003), no. 6, 425–430.

[3] Ph. Angot, A unified fictitious domain model for general embedded boundary conditions, C. R. Acad. Sci. Paris, Serie I Math. 341 (2005), no. 11, 683–688.

[4] Ph. Angot, A fictitious domain model for the Stokes/Brinkman problem with jump embedded boundary conditions, C. R. Math. Acad. Sci. Paris, Serie I 348 (2010), no. 11-12, 697–702.

[5] Ph. Angot, On the well-posed coupling between free fluid and porous viscous flows, Appl. Math. Lett. 24 (2011), no. 6, 803–810.

[6] Ph. Angot, G. Carbou, and V. Péron, Asymptotic study for Stokes-Brinkman model with jump embedded transmission conditions, Asymptotic Analysis 96 (2016), no. 3-4, 223–249.

[7] J. T. Beale and A. T. Layton, On the accuracy of finite difference methods for elliptic problems with interfaces, Commun. Appl. Math. Comput. Sci. 1 (2006), 91–119.

[8] H. Brezis, Functional analysis, Sobolev spaces and Partial Differential Equations, Springer-Verlag (New York), 2011.

[9] P. Grisvard, Elliptic problems in nonsmooth domains, Monographs and Studies in Math., vol. 24, Pitman (London), 1985.

[10] Z. Li, A fast iterative algorithm for elliptic interface problems, SIAM J. Numer. Anal. 35 (1998), 230–254.

[11] Z. Li, IIMPACK: A collection of fortran codes for interface problems, Anonymous ftp at ftp.ncsu.edu under the directory: /pub/math/zhilin/Package and http://www4.ncsu.edu/~zhilin/IIM, last updated: 2008.

[12] Z. Li and K. Ito, Maximum principle preserving schemes for interface problems with discontinuous coefficients, SIAM J. Sci. Comput. 23 (2001), 1225–1242.

[13] Z. Li and K. Ito, The immersed interface method – numerical solutions of pdes involving interfaces and irregular domains, SIAM Frontier Series in Applied mathematics, FR33, 2006.

[14] Z. Li, H. Ji, and X. Chen, Accurate solution and gradient computation for elliptic interface problems with variable coefficients, SIAM J. Numer. Anal. 55(2) (2017) 570-597.

[15] J. Nečas, Les méthodes directes en théorie des équations elliptiques, Masson (Paris), 1967.

[16] C. S. Peskin, The Immersed Boundary Method, Acta Numerica (2002), 479–517.

[17] I. Ramière, Ph. Angot, and M. Belliard, A fictitious domain approach with spread interface for elliptic problems with general boundary conditions, Comput. Meth. in Appl. Mech. and Engrng. 196 (2007), no. 4-6, 766–781.

[18] I. Ramière, Ph. Angot, and M. Belliard, A general fictitious domain method with immersed jumps and multilevel nested structured meshes, J. Comput. Phys. 225 (2007), no. 2, 1347–1387.

[19] J. Xia and Z. Li, Effective matrix-free preconditioning for the augmented immersed interface method, preprint, 2014.

[1] Aix-Marseille Université, Institut de Mathématiques de Marseille, CNRS UMR-7373, Centrale Marseille, 13453 Marseille, France

E-mail: `philippe.angot@univ-amu.fr`

[2] Center for Research in Scientific Computation (CRSC) and Department of Mathematics North Carolina State University (NCSU), Raleigh, USA

E-mail: `zhilin@math.ncsu.edu`